

Cross-linking of C-terminal Residues of Phospholamban to the Ca²⁺ Pump of Cardiac Sarcoplasmic Reticulum to Probe Spatial and Functional Interactions within the Transmembrane Domain*

Received for publication, February 10, 2006, and in revised form, March 15, 2006. Published, JBC Papers in Press, March 22, 2006, DOI 10.1074/jbc.M601338200

Zhenhui Chen[‡], Brandy L. Akin[‡], David L. Stokes^{§¶}, and Larry R. Jones^{‡¶1}

From the [‡]Krannert Institute of Cardiology and the Department of Medicine, Indiana University School of Medicine, Indianapolis, Indiana 46202, the [§]Skirball Institute of Biomolecular Medicine, New York University School of Medicine, New York, New York 10016, and the [¶]New York Structural Biology Center, New York, New York 10027

Interactions between the transmembrane domains of phospholamban (PLB) and the cardiac Ca²⁺ pump (SERCA2a) have been investigated by chemical cross-linking. Specifically, C-terminal, transmembrane residues 45–52 of PLB were individually mutated to Cys, then cross-linked to V89C in the M2 helix of SERCA2a with the thiol-specific cross-linking reagents Cu²⁺-phenanthroline, dibromobimane, and bismaleimido-hexane. V49C-, M50C-, and L52C-PLB all cross-linked strongly to V89C-SERCA2a, coupling to 70–100% of SERCA2a molecules. Residues 45–48 and 51 of PLB also cross-linked to V89C of SERCA2a, but more weakly. Evidence for the mechanism of PLB regulation of SERCA2a was provided by the conformational dependence of cross-linking. In particular, the required absence of Ca²⁺ for cross-linking implicated the E2 conformation of SERCA2a, and its enhancement by ATP confirmed E2·ATP as the conformation with the highest affinity for PLB. In contrast, E2 phosphorylated with inorganic phosphate (E2P) and E2 inhibited by thapsigargin (E2·TG) both failed to cross-link to PLB. These results with transmembrane PLB residues are completely consistent with cytoplasmic PLB residues studied previously, suggesting that the dissociation of PLB from the Ca²⁺ pump is complete, not partial, when the pump binds Ca²⁺ (E1·Ca_i) or adopts the E2P or E2·TG conformations. V49C of PLB cross-linked to 100% of SERCA2a molecules, suggesting that this residue might have functional importance for regulation. Indeed, we found that mutation of Val⁴⁹ to smaller side-chained residues V49A or V49G augmented PLB inhibition, whereas mutation to the larger hydrophobic residue, V49L, prevented PLB inhibition. A model for the interaction of PLB with SERCA2a is presented, showing that Val⁴⁹ fits into a constriction at the luminal end of the M2 helix of SERCA, possibly controlling access of PLB to its binding site on SERCA.

Phospholamban (PLB)² is a small membrane protein of only 52 amino acids, and serves as a key regulator of myocardial contractile kinetics

(1–3). This regulation involves physical binding of PLB to the SERCA2a isoform of Ca²⁺-ATPase (4–7), the Ca²⁺ pump found in cardiac SR, which is responsible for actively transporting Ca²⁺ into the SR lumen to maintain SR Ca²⁺ stores. In particular, dephosphorylated PLB decreases the apparent affinity of the Ca²⁺ pump for Ca²⁺ by slowing the E2 to E1 transition of the catalytic cycle that couples ATP hydrolysis to Ca²⁺ transport (8). Upon phosphorylation, this inhibitory effect of PLB on SERCA2a Ca²⁺ affinity is reversed, resulting in increased Ca²⁺ transport into the SR and in stronger heart contraction and relaxation, thus producing the so-called positive inotropic and lusitropic effects of β-adrenergic stimulation (1, 2). PLB contains two major domains, a regulatory, cytoplasmic domain I (residues 1–31), and an anchoring, transmembrane domain II (residues 32–52). At the cytoplasmic domain, several residues are important for PLB inhibitory function (9, 10). For example, Ser¹⁶ and Thr¹⁷ located in domain IA (residues 1–20) represent the phosphorylation sites for cAMP-dependent protein kinase and Ca²⁺/CaM protein kinase, respectively. Phosphorylation at either site reverses PLB inhibition (1). Moreover, Asn²⁷, Asn³⁰, and Leu³¹ in domain IB (residues 21–31) are directly involved in the physical interaction with SERCA2a (4–7), and mutation here can drastically enhance or attenuate PLB inhibitory function (10, 11). Domain II of PLB, the transmembrane domain, contains a heptad repeat of Leu/Ile residues on one face of the helix that participate in a coiled-coil interaction to form a PLB homopentamer (12). Changes to these residues produce monomeric PLB, which is believed to be the active form that binds to SERCA2a and inhibits its Ca²⁺ transport cycle (11, 13). Mutation of residues along the transmembrane helix of PLB can also enhance or attenuate PLB inhibitory function depending on location, and several amino acids distributed throughout the entire length of the helix appear to be directly involved in binding to SERCA2a (6, 7, 11, 14).

By use of chemical cross-linking reagents, we recently identified several sites of interaction between key residues in domain IB of PLB and residues at the cytoplasmic extension of M4 of SERCA2a (4–6). Specifically, two gain-of-function mutants, N27C-PLB and N30C-PLB, cross-linked strongly to Lys³²⁸ of the M4 helix of SERCA2a with use of the heterobifunctional Cys to Lys cross-linking agents *N*-(ε-maleimido-caproyloxy)succinimide ester (EMCS) and KMUS, respectively (5). Furthermore, the homobifunctional sulfhydryl cross-linking agent, BMH, coupled both the gain of function mutant N30C-PLB and the loss of function mutant L31C-PLB to Cys³¹⁸ (4) and T317C (6) of the SERCA2a M4 helix, respectively, thus identifying domain IB of PLB as an important site of physical and functional interaction with residues in M4 of SERCA2a. Cross-linking between PLB and SERCA2a at all these interaction sites was inhibited by micromolar Ca²⁺ or by TG, but stimulated

* This work was supported by National Institutes of Health Grants HL49428 (to L. R. J.) and GM56960 (to D. L. S.). The costs of publication of this article were defrayed in part by the payment of page charges. This article must therefore be hereby marked "advertisement" in accordance with 18 U.S.C. Section 1734 solely to indicate this fact.

¹ To whom correspondence should be addressed: 1800 N. Capitol Ave., Indianapolis, IN 46202. Tel.: 317-962-0095 Fax: 317-962-0113; E-mail: lrjones@iupui.edu.

² The abbreviations used are: PLB, phospholamban; SR, sarcoplasmic reticulum; SERCA2a, isoform of Ca²⁺-ATPase in cardiac SR; SERCA1a, isoform of Ca²⁺-ATPase in fast twitch skeletal muscle; MOPS, 3-(*N*-morpholino)propanesulfonic acid; M, transmembrane domain; E1, high Ca²⁺ affinity conformation of Ca²⁺-ATPase; E2, low Ca²⁺ affinity conformation of Ca²⁺-ATPase; E2P, E2 with covalently bound P_i at Asp³⁵¹; K_{Ca}, Ca²⁺ concentration required for half-maximal effect; K_{ATP}, ATP concentration required for half-maximal effect; TG, thapsigargin; BMH, 1,6-bismaleimido-hexane; bBB, dibromobimane; KMUS, *N*-(κ-maleimido-dodecanoyloxy)sulfosuccinimide ester; LDS, lithium dodecyl sulfate; Me₂SO, dimethyl sulfoxide; WT, wild-type.

Transmembrane Residues of PLB Binding to E2-ATP

by the nucleotides ATP or ADP in the absence of Ca^{2+} (4–6). Based on these results, we proposed that domain IB residues of PLB interact with SERCA2a only in Ca^{2+} -free, E2 conformation, preferably with bound nucleotide. Interestingly, the TG used to stabilize this E2 conformation for structural studies (15) prevented PLB interaction, suggesting that TG induces a unique, non-physiological conformation. Another recent study also showed cross-linking of N27C and N30C of PLB to L321C of the skeletal muscle Ca^{2+} pump (SERCA1a) using Cu^{2+} -phenanthroline (7), consistent with this cytoplasmic interaction region.

Val⁴⁹ is in the transmembrane helix at the C-terminal end of PLB and appears to be an important residue for PLB function. An earlier study suggested that Ala replacement at Val⁴⁹ results in nearly complete loss of the PLB inhibitory function (11). Subsequently, this proposed loss-of-function PLB mutant (V49A-PLB) was used as a dominant-negative probe to reverse WT-PLB inhibition of SERCA2a in failed cardiac cells, and to restore normal cardiomyocyte function in a mouse model of heart failure (16). In contrast, when a similar mutant, V49G-PLB, was made, gain of PLB function, not loss of function was reported (17). V49G-PLB caused very strong SERCA2a inhibition, and in fact induced heart failure when overexpressed in the ventricles of transgenic mice (17). These apparently contradictory results suggest an important functional role for Val⁴⁹ of PLB, but highlight the need to clarify the exact role and mechanism of Val⁴⁹ in overall SERCA2a inhibition. Recently, Toyoshima *et al.* (7) reported successful cross-linking of V49C-PLB to V89C-SERCA1a (skeletal muscle isoform) with use of Cu^{2+} -phenanthroline (7), which demonstrated for the first time the close proximity between the C-terminal end of PLB and Val⁸⁹ in the M2 helix of SERCA.

In the work reported here, we have extended our cross-linking approach to examine physical and functional interactions between the C-terminal end of PLB (residues 45–52) and V89C in the M2 helix of SERCA2a, taking advantage of the recent observation of Toyoshima *et al.* (7) that coupling can occur here between PLB and SERCA. Results obtained after cross-linking of eight residues at the membrane terminus of PLB are remarkably consistent with results obtained previously after cross-linking of the cytoplasmic domain IB residues of PLB to residues at the cytoplasmic extension of M4 (4–6). At both domains, PLB cross-links to SERCA2a preferentially in the nucleotide-bound, E2 conformation. Thus, Ca^{2+} binding by SERCA2a, which stabilizes E1, appears to induce a global dissociation of PLB that accounts for the relief of inhibition, and PLB appears to recognize a single, unique conformation of SERCA2a: E2 stabilized by bound nucleotide. Contrary to previous reports with Val⁴⁹ (11, 16), we show that a hydrophobic side chain here actually interferes with PLB inhibition. The structural role of Val⁴⁹ in the context of SERCA2a inhibition is discussed.

EXPERIMENTAL PROCEDURES

Materials—The cross-linkers BMH and KMUS were obtained from Pierce, and bBBR was purchased from Molecular Probes. Thapsigargin, phenanthroline, and Me_2SO were purchased from Sigma. $^{32}\text{P}_i$ was obtained from PerkinElmer Life Sciences.

Mutagenesis and Baculovirus Production—Mutation of canine SERCA2a and PLB cDNAs was conducted as recently described (4–6). V89C-SERCA2a was made directly in the transfection vector pVL1393 using the QuikChangeTM XL-Gold system (Stratagene) (4–6). For cross-linking studies, the Cys-scanning point mutants of PLB, I45C, A46C, I47C, I48C, V49C, M50C, L51C, and L52C were made on the Cys-less PLB background, which is a fully functional canine PLB with Cys residues 36, 41, and 46 changed to Ala (4–6). For the Ca^{2+} -ATPase assays depicted in Fig. 7 and Table 2, the V49A, V49G, V49C, and V49L mutations of PLB were made on the WT-PLB background

(Cys³⁶, Cys⁴¹, and Cys⁴⁶ remaining intact) to facilitate comparisons with previous work by others (11, 16, 17). All mutated cDNAs were confirmed by DNA sequencing of the plasmid vectors, then re-confirmed in the final viral vectors after PCR amplification of the mutated region. Baculoviruses encoding mutated proteins were generated as previously described with BaculoGoldTM (BD Pharmingen) linearized baculovirus DNA (4–6).

Protein Expression—Sf21 insect cells were co-infected with baculoviruses encoding WT and mutated proteins as recently described (4–6). Microsomes were harvested after 60 h co-infection and stored frozen in small aliquots at -40°C at a protein concentration of 6–10 mg/ml in 0.25 M sucrose, 10 mM MOPS (pH 7.0). Protein assay was by the Lowry method (13). PLB was expressed at $\sim 4:1$ molar ratio to SERCA2a (4–6, 13).

Ca^{2+} -ATPase Assay— Ca^{2+} -ATPase activity was assayed at 37°C in buffer containing 50 mM MOPS (pH 7.0), 3 mM MgCl_2 , 100 mM KCl, 1 mM EGTA, 5 mM NaN_3 , and 3 $\mu\text{g}/\text{ml}$ of the Ca^{2+} ionophore, A23187 (13). Ionized calcium concentrations were set by addition of CaCl_2 . Ca^{2+} -ATPase activities were measured in the presence and absence of anti-PLB monoclonal antibody, 2D12, which reverses PLB inhibition (4). For each preparation, maximal Ca^{2+} -ATPase activity was also determined in the presence of 50 μM added Ca^{2+} with no added EGTA, an ionized Ca^{2+} concentration that totally reverses PLB inhibition (8, 13). The amount of microsomal protein used for cross-linking and $^{32}\text{P}_i$ labeling experiments was then adjusted for small variations in amounts of Ca^{2+} pump protein expressed between preparations, based on the maximal Ca^{2+} -ATPase activities determined. Maximal Ca^{2+} -ATPase activities ranged between 10 and 15 μmol of P_i/mg of protein/h for all preparations used in this study. All ATPase activities reported are Ca^{2+} -dependent (13).

Cross-linking—Cross-linking between Cys residues of PLB in domain II and V89C of SERCA2a in M2 was conducted using the homobifunctional thiol cross-linking reagents BMH or bBBR, or with Cu^{2+} -phenanthroline. Reactions were conducted with 10–15 μg of microsomal protein (adjusted for equivalent amounts of SERCA2a expressed, see above) in 12 μl of E2 buffer, which contained 40 mM MOPS (pH 7.0), 3.2 mM MgCl_2 , 75 mM KCl, 3 mM ATP, and 1 mM EGTA. In Fig. 3, ionized calcium concentrations were set by adding CaCl_2 . In some experiments, ATP concentration was varied, as indicated. TG was added from stock solutions in ethanol. Cross-linking reactions were started by adding 0.75 μl of bBBR or BMH from 1.6 mM stock solutions in Me_2SO (0.1 mM final cross-linker concentrations), or by adding 0.75 μl of CuSO_4 and phenanthroline to yield final concentrations of 0.3 and 0.9 mM, respectively. Reactions were conducted at room temperature for 10 min with BMH or Cu^{2+} -phenanthroline, and for 1 h at room temperature with bBBR. N30C-PLB was cross-linked to Lys³²⁸ of wild-type SERCA2a for 10 min at room temperature using the heterobifunctional cross-linking agent KMUS, in an identical system (5). Reactions were stopped by adding 7.5 μl of SDS-PAGE sample loading buffer, which contained 15% SDS, 100 mM dithiothreitol (omitted when Cu^{2+} -phenanthroline was used), 20% glycerol, 62 mM Tris (pH 6.8), and a trace of bromphenol blue as a tracking dye. After terminating the reactions, samples were subjected to SDS-PAGE (18) followed by immunoblotting with anti-PLB monoclonal antibody, 2D12, to detect PLB cross-linked to SERCA2a (4–6). Antibody visualization was with ^{125}I -protein A.

Phosphorylation of SERCA2a with $^{32}\text{P}_i$ —In some experiments, simultaneous cross-linking of SERCA2a to PLB and phosphorylation of SERCA2a with $^{32}\text{P}_i$ to form E2P was performed. In these experiments, 12 μl of E2 buffer was replaced with 12 μl of buffer promoting E2P formation, which consisted of 40 mM MOPS (pH 7.0), 20 mM MgCl_2 , 20% Me_2SO , 1.0 mM EGTA, and 0.25 mM radioactive or non-radioactive

P_i (E2P buffer). ATP concentration was varied as indicated. Reactions were started by adding 10–15 μg of microsomal protein containing equivalent amounts of SERCA2a per reaction tube, and after a 10-min incubation at room temperature to allow E2P formation, cross-linking of different PLB mutants to SERCA2a was initiated by adding cross-linkers as described above to two duplicate sets of reaction tubes, one containing non-radioactive P_i , and the other $^{32}\text{P}_i$. For assessment of cross-linking, one set of reaction tubes, which had been incubated with 0.25 mM non-radioactive P_i , was terminated and processed identically as described above. For measurement of E2P formation, a duplicate set of reaction tubes, which had been incubated with 0.25 mM $^{32}\text{P}_i$, was terminated by adding 7.5 μl of LDS sample loading buffer per tube, which contained 200 mM glycine (pH 2.4), 20% glycerol, 3% LDS, 100 mM dithiothreitol, and a trace of malachite green as the tracking dye. Gel electrophoresis in 7% polyacrylamide under acidic conditions to retain E2P was then performed by the following method modified from Lichtner and Wolf (19). A polyacrylamide gel was polymerized the day before the experiment using ascorbic acid/ $\text{FeSO}_4/\text{H}_2\text{O}_2$ (19) in gel buffer consisting of 0.1 M Tris/HCl, 0.3 M glycine, and 0.1% LDS (pH 2.4). The upper and lower tank buffers were identical to the gel buffer. On the day of the experiment, the LDS-solubilized membranes were loaded directly on the polymerized gel and electrophoresis was conducted at 200 mA at 4 °C for 4 h. The gel was then stained with Coomassie Blue in 10% acetic acid, 25% isopropyl alcohol for 1 h, destained with several changes of 10% acetic acid, 25% isopropyl alcohol for 3 h, and dried overnight using a Bio-Rad GelAir Dryer.

$^{32}\text{P}_i$ bands in dried polyacrylamide gels and ^{125}I bands on nitrocellulose sheets were visualized by autoradiography, then quantified with a Bio-Rad Personal Fx phosphorimager. Data analysis was done with Origin (Microcal).

RESULTS

Chemical Coupling between V49C-PLB and V89C-SERCA2a with Cu^{2+} -phenanthroline and Dibromobimane—We previously reported highly specific cross-linking between residues in cytoplasmic domain IB of PLB and residues in the cytoplasmic extension of M4 of SERCA2a (4–6), after the two proteins were functionally co-expressed in insect cell microsomes. In this study, we shifted our attention to cross-linking interactions between the C-terminal end of PLB encompassing residues 45–52 and potential residues of SERCA2a. The last 8 residues of PLB, Ile⁴⁵ to Leu⁵², located at the luminal side of the SR membrane bilayer were individually mutated to Cys, and the mutated PLB molecules were co-expressed with WT-SERCA2a in insect cell microsomes. Mutations were made on the Cys-less PLB background, which retains full functional activity. All these PLB mutants inhibited WT-SERCA2a by increasing the K_{Ca} of Ca^{2+} -activated ATPase activity, demonstrating that they were functionally intact (data not shown). However, none of these Cys-scanning mutants of PLB cross-linked to WT-SERCA2a with use of a series of homobifunctional or heterobifunctional cross-linking agents tested previously on domain IB mutants of PLB (4, 5), probably due to the lack of endogenous Cys or Lys residues in SERCA2a that were in proximity to the mutated PLB residues (data not shown).

Toyoshima *et al.* (7) recently reported successful cross-linking of V49C-PLB to V89C of the skeletal muscle Ca^{2+} pump (SERCA1a) with use of Cu^{2+} -phenanthroline, a zero-length sulfhydryl cross-linking agent. Fig. 1, lane 5, confirms the results with the cardiac Ca^{2+} pump (SERCA2a), by showing the strong cross-linking of V49C of PLB to V89C in the M2 helix of SERCA2a after co-expression of both proteins in insect cell microsomes. Although not previously reported, V89C-SERCA retained similar enzymatic activity as WT-SERCA with identi-

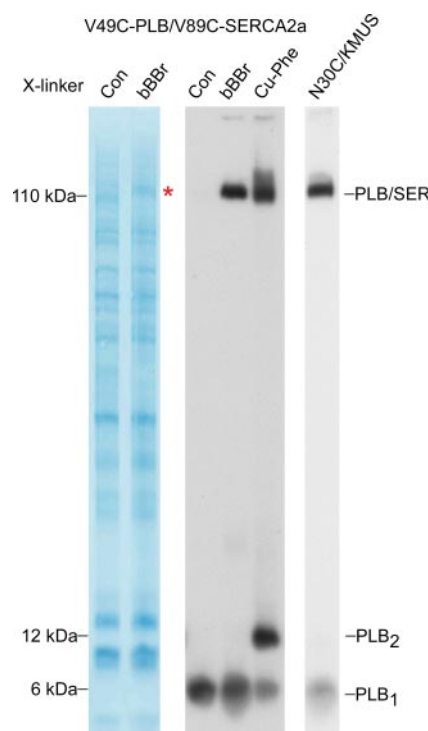


FIGURE 1. Cross-linking of V49C-PLB to V89C-SERCA2a. Insect cell microsomes co-expressing V49C-PLB and V89C-SERCA2a (left and middle panels), or N30C-PLB and WT-SERCA2a (right panel), were incubated in E2 buffer with bBBR for 1 h, or Cu^{2+} -phenanthroline (Cu-Phe) or 0.1 mM KMUS for 10 min at room temperature. Cross-linkers (X-linker) used are indicated at the top, with control (Con) no added cross-linker. Reactions were stopped by adding SDS-PAGE sample loading buffer. Samples were subjected to SDS-PAGE, transferred to nitrocellulose, and stained with Amido Black (left panel), followed by incubation with anti-PLB antibody and ^{125}I -protein A (middle and right panels). The red asterisk shows the Amido Black-stained Ca^{2+} -ATPase (110 kDa) shifted upwards on the nitrocellulose sheet, after cross-linking to PLB with bBBR. PLB/SER, PLB cross-linked to SERCA2a; PLB₁ and PLB₂, PLB monomer and dimer.

TABLE 1
Effects of domain II mutants of PLB on apparent Ca^{2+} affinity of V89C-SERCA2a

WT-SERCA2a, V89C-SERCA2a, or V89C-SERCA2a plus WT-PLB or the different PLB mutants indicated were expressed in Sf21 cells, followed by measurement of Ca^{2+} -ATPase activities in membranes in the presence and absence of anti-PLB monoclonal antibody, 2D12 (\pm Ab). K_{Ca} values (μM) for Ca^{2+} activation of ATP hydrolysis are reported. All PLB mutants were co-expressed on the Cys-less PLB background, which is WT-PLB with Cys³⁶, Cys⁴¹, and Cys⁴⁶ changed to Ala. Results are the means \pm S.D. from three to six preparations.

Protein expressed	K_{Ca} values	
	–Antibody	+Antibody
WT-SERCA2a	0.14 \pm 0.02	0.14 \pm 0.02
V89C-SERCA2a	0.12 \pm 0.01	0.12 \pm 0.02
+WT-PLB	0.21 \pm 0.03	0.15 \pm 0.02
+I45C-PLB	0.21 \pm 0.02	0.15 \pm 0.01
+Cys ⁴⁶ -PLB	0.23 \pm 0.03	0.14 \pm 0.02
+I47C-PLB	0.23 \pm 0.04	0.13 \pm 0.01
+I48C-PLB	0.19 \pm 0.01	0.13 \pm 0.01
+V49C-PLB	0.28 \pm 0.03	0.15 \pm 0.02
+M50C-PLB	0.21 \pm 0.04	0.14 \pm 0.02
+L51C-PLB	0.25 \pm 0.01	0.16 \pm 0.01
+L52C-PLB	0.24 \pm 0.01	0.13 \pm 0.00

cal apparent Ca^{2+} affinity (Table 1). Moreover, V89C-SERCA2a retains the ability to be inhibited by PLB (Table 1). The apparent Ca^{2+} affinity for ATP hydrolysis by V89C-SERCA2a was decreased after co-expression with WT-PLB, and inhibition was reversed by addition of the anti-PLB monoclonal antibody, 2D12, which mimics the effect of PLB phosphorylation at Ser¹⁶ in preventing PLB inhibition (20) (Table 1). Interestingly, V49C-PLB, which cross-links to V89C-SERCA2a, was a

Transmembrane Residues of PLB Binding to E2-ATP

more effective SERCA2a inhibitor than WT-PLB, shifting the K_{Ca} value for ATP hydrolysis from 0.12 to 0.28 μM , as compared with 0.21 μM for WT-PLB (Table 1).

The cross-linking between V49C-PLB and V89C-SERCA2a was examined in more detail. Of numerous homobifunctional thiol cross-linking agents tested, the shortest, bBBr (cross-linking distance 5 Å) (21), was as efficient as Cu^{2+} -phenanthroline in promoting V49C-PLB to V89C-SERCA2a coupling (Fig. 1, lane 4). Cu^{2+} -phenanthroline dimerized PLB monomers (PLB_2), whereas bBBr did not (PLB_1). Unlike the previous results of Toyoshima *et al.* (7), we observed no spontaneous cross-linking between V49C-PLB and V89C-SERCA2a in the absence of cross-linking agents (Fig. 1, lane 3). Among numerous protein bands visible on the Amido Black-stained nitrocellulose blot, only the mobility of SERCA2a (110 kDa) was shifted upwards after addition of bBBr (Fig. 1, lane 2, asterisk). This mobility shifted band was identified as the cross-linked heterodimer of V49C-PLB and V89C-SERCA2a (lane 4), demonstrating the high specificity of the PLB to SERCA2a cross-linking interaction in insect cell microsomal membranes. In fact, virtually 100% of the expressed V89C-SERCA2a molecules were cross-linked to V49C of PLB by bBBr (or Cu^{2+} -phenanthroline), similar to our earlier cross-linking of N30C-PLB in domain IB to Lys³²⁸ of WT-SERCA2a using the heterobifunctional cross-linking agent, KMUS (5) (Fig. 1, lane 6). Cross-linking between V49C-PLB and V89C-SERCA2a with use of Cu^{2+} -phenanthroline reached the maximum level by a 10-min incubation at room temperature. Cross-linking of V49C-PLB to V89C-SERCA2a by bBBr was slower, with a $t_{1/2}$ of 30 min at room temperature. In the following experiments, we examined cross-linking at other domain II residues of PLB, and express results as percentages of Ca^{2+} -ATPase molecules cross-linked for each PLB mutant under the conditions specified.

Chemical Coupling between Residues 45 and 52 of PLB and V89C-SERCA2a—Cys-scanning mutagenesis was used to probe with higher resolution the proximity between all of the C-terminal residues (residues 45–52) of PLB and V89C of SERCA2a, using the thiol cross-linking agents Cu^{2+} -phenanthroline (zero length cross-linker), bBBr (5 Å long), and BMH (10 Å long) as molecular rulers. In control experiments, we observed that all of these PLB mutants inhibited SERCA2a activity by increasing K_{Ca} values for activation of Ca^{2+} -ATPase activity, and that inhibition was reversed by the anti-PLB antibody, 2D12 (Table 1). Similar to V49C-PLB, a 10-min incubation with Cu^{2+} -phenanthroline also cross-linked L52C-PLB to a substantial fraction (45%) of V89C-SERCA2a molecules, as well as I48C-PLB, M50C-PLB, and L51C-PLB to V89C-SERCA2a with lower efficiencies (24, 10, and 12%, respectively) (Fig. 2A). On the other hand, I45C-, Cys⁴⁶-, and I47C-PLB did not cross-link to V89C-SERCA2a with Cu^{2+} -phenanthroline (Fig. 2A). These results suggest that Val⁴⁹ and Leu⁵² of PLB are located on the same side of the transmembrane α -helix of PLB in close proximity to V89C of SERCA2a, where they are poised for efficient, zero-length cross-linking.

Cross-linking obtained with bBBr (Fig. 2B), the shorter of the two homobifunctional cross-linking agents, was similar to cross-linking with Cu^{2+} -phenanthroline, although longer incubation times were required, as noted above. Again, cross-linking of V49C-PLB to V89C-SERCA2a was the strongest and reached 100% of pump molecules cross-linked after a 1-h room temperature incubation. L52C also cross-linked strongly to V89C-SERCA2a with bBBr (67%), followed by I48C, M50C, and L51C at 38, 30, and 26%, respectively. 11% or fewer Ca^{2+} pumps were cross-linked for the other Cys mutants with use of bBBr (Fig. 2B). Thus, although the patterns of cross-linking obtained with Cu^{2+} -phenanthroline and bBBr were similar, the use of the slightly longer bBBr enabled a wider range of PLB residues to be covalently

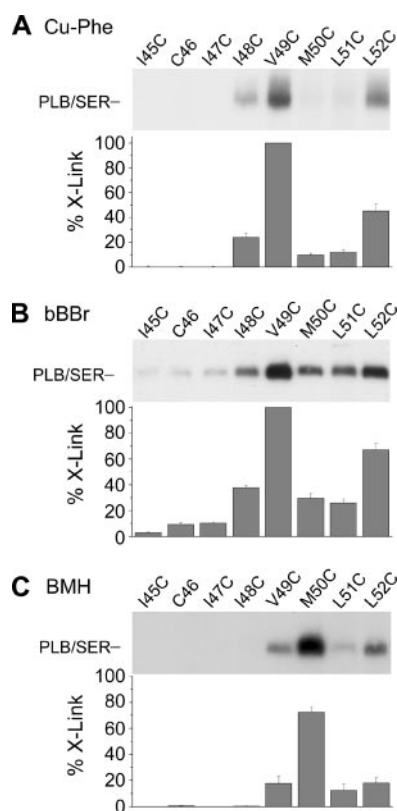


FIGURE 2. Cross-linking efficiencies of C-terminal residues of PLB to V89C-SERCA2a. I45C- through L52C-PLB (expressed on the Cys-less PLB background) were co-expressed with V89C-SERCA2a and cross-linked to V89C-SERCA2a in E2 buffer with the cross-linkers indicated in panels A–C. Cross-linking with Cu^{2+} -phenanthroline and BMH was conducted for 10 min at room temperature, and with bBBr for 1 h at room temperature. The upper immunoblots of each panel show representative cross-linking results scanning the entire PLB region, and the lower bar graphs show the percentages of Ca^{2+} pumps cross-linked to each PLB mutant ($n = 4–6$ for each PLB mutant).

attached to V89C of SERCA2a. Although the efficiencies of these extra bBBr couplings were lower, they remained specific and responded identically to different allosteric factors (see below).

BMH, with the longer spacer arm of 10 Å, gave a completely different pattern of cross-linking (Fig. 2C). BMH only cross-linked the last 4 residues of PLB to V89C-SERCA2a, but with significant differences depending upon which PLB residue was mutated. M50C-PLB cross-linked the strongest and the fastest to V89C-SERCA2a, coupling to 72% of Ca^{2+} pump molecules after a 10-min incubation. In contrast, V49C-PLB, L51C-PLB, and L52C-PLB cross-linked to $\leq 18\%$ of V89C-SERCA2a molecules after a 10-min incubation with BMH, although they were able to reach a maximum coupling efficiency of about 50% after a 1-h incubation (data not shown). These results with BMH suggest that Met⁵⁰ of PLB is located on the opposite side of the PLB helix from Val⁴⁹ and Leu⁵², where it cross-links to V89C of SERCA2a most efficiently at a distance of 10 Å.

We noted that cross-linking with Cu^{2+} -phenanthroline, which catalyzes disulfide bond formation, gave “fuzzier” PLB/SER signals compared with use of bBBr or BMH for protein cross-linking (Figs. 1 and 2), and, moreover, frequently led to variable results and protein aggregation visible at the tops of the gels. To retain the disulfide bonds formed, dithiothreitol was omitted during processing of Cu^{2+} -phenanthroline cross-linked samples, which appeared to account for much of the protein aggregation observed. Nonspecific aggregation of SERCA by Cu^{2+} -phenanthroline has been noted previously (22). For these reasons, V89C of SERCA2a was cross-linked to PLB with bBBr or BHM in the remaining experiments unless otherwise stated.

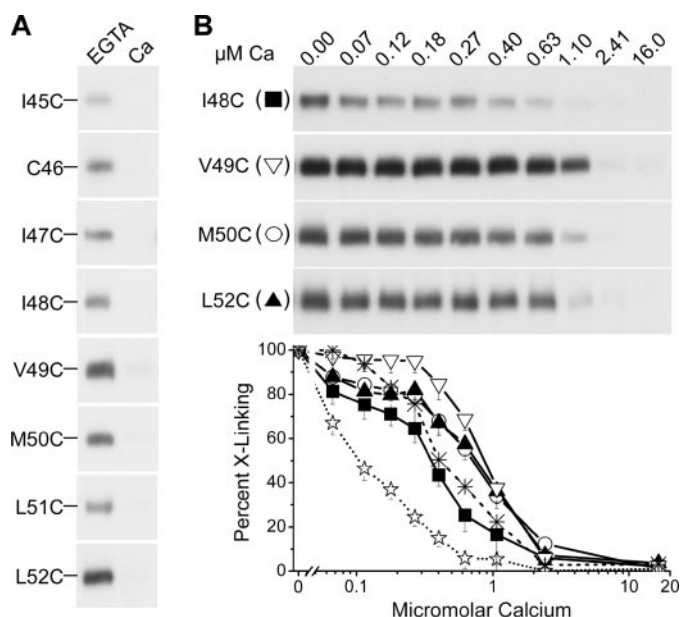


FIGURE 3. Ca^{2+} inhibition of cross-linking of residues 45–52 of PLB to V89C-SERCA2a. I45C through V49C-PLB, L51C, and L52C-PLB were cross-linked to V89C-SERCA2a for 1 h at room temperature with bBBr. M50C-PLB was cross-linked to V89C-SERCA2a for 10 min at room temperature with BMH. *A* shows PLB cross-linked to V89C-SERCA2a when cross-linking was conducted in E2 buffer containing 1 mM EGTA with no added Ca^{2+} (EGTA), or in E2 buffer containing 10 μM added Ca^{2+} , with no EGTA (*Ca*). *B*, Ca^{2+} concentration effects on cross-linking. Upper immunoblots show ionized Ca^{2+} concentration dependence on inhibition of cross-linking of I48C-, V49C-, M50C-, and L52C-PLB to V89C-SERCA2a in E2 buffer. The lower graph plots Ca^{2+} inhibition of cross-linking of PLB mutants in *B* normalized to 100% cross-linking in the absence of Ca^{2+} . Cross-linking of N30C-PLB to WT-SERCA2a with BMH (dotted line) and KMUS (dashed line) was also measured as described in the text ($n = 3-6$ for each mutant).

Ca²⁺ Inhibition of Cross-linking at Transmembrane Domain Residues of PLB—Similar to previous cross-linking between domain IB residues of PLB and the cytoplasmic extension of M4 of SERCA2a (4–6), cross-linking of PLB domain II residues to M2 of SERCA2a was totally inhibited by 10 μM Ca^{2+} (Fig. 3A). These results suggest that the C-terminal, transmembrane residues 45–52 of PLB also bind to SERCA2a only when it is in the Ca^{2+} -free, E2 conformation. It should be pointed out that none of these PLB mutants inhibited Ca^{2+} -ATPase activity at 10 μM Ca^{2+} (Table 1), consistent with complete dissociation of PLB from SERCA2a molecules under maximal Ca^{2+} transport conditions (4–6).

Ca^{2+} inhibition curves on cross-linking were performed for the four strongest cross-linking residues of PLB at domain II, I48C, V49C, M50C, and L52C. K_{Ca} values for Ca^{2+} inhibition of cross-linking at these PLB residues to V89C of SERCA2a varied in the low micromolar range between 0.3 and 0.9 μM Ca^{2+} (Fig. 3B). The K_{Ca} value for cross-linking of I48C-PLB to V89C-SERCA2a ($0.36 \pm 0.04 \mu\text{M}$) was similar to that previously reported for cross-linking of N30C-PLB to Lys³²⁸ of WT-SERCA2a (5). However, K_{Ca} values for inhibition of cross-linking of V49C-PLB ($0.87 \pm 0.05 \mu\text{M}$), M50C-PLB ($0.68 \pm 0.09 \mu\text{M}$), and L52C-PLB ($0.78 \pm 0.15 \mu\text{M}$) to V89C-SERCA2a were somewhat higher, but still within the range at which PLB inhibits SERCA2a activity. Interestingly, cross-linking of N30C of PLB to Cys³¹⁸ of SERCA2a in domain IB by BMH was the most sensitive to Ca^{2+} (Fig. 3B, dotted line), with a K_{Ca} value of $0.11 \pm 0.02 \mu\text{M}$ for cross-linking inhibition as noted previously (4). The different K_{Ca} values obtained in the low micromolar range for inhibition of cross-linking may reflect the subdomain motion of the Ca^{2+} pump associated with Ca^{2+} binding, imparting subtle differences in cross-linking efficiencies depending on cross-linker length and steric factors. It is also possible that PLB could “peel off” differentially from

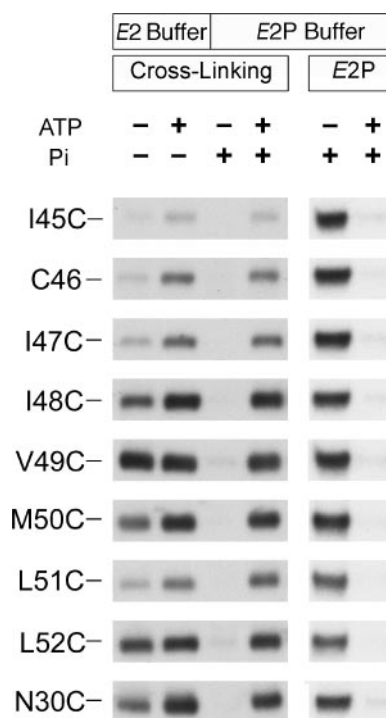


FIGURE 4. ATP and P_i effects on cross-linking. I45C through L52C-PLB were cross-linked to V89C-SERCA2a with bBBr or BHM as described in the legend to Fig. 3. N30C-PLB was cross-linked to WT-SERCA2a with KMUS as described in the legend to Fig. 1. 3 mM ATP or 0.25 mM P_i were included as shown (top). For E2P formation, membranes were preincubated for 10 min at room temperature with non-radioactive P_i (lanes 3 and 4) or $^{32}\text{P}_i$ (lanes 5 and 6), prior to addition of cross-linkers. Lanes 1–4 show cross-linking results obtained in the two Ca^{2+} -free buffers (top), E2 buffer or E2P buffer. Lanes 5 and 6 are $^{32}\text{P}_i$ autoradiograms showing E2P formation in E2P buffer.

SERCA2a in different regions when the enzyme binds Ca^{2+} . Toyoshima *et al.* (7) reported that 10 mM Ca^{2+} partially inhibits Cu^{2+} -phenanthroline catalyzed cross-linking of V49C-PLB to V89C of SERCA1a, but effects of Ca^{2+} in the micromolar range were not cited. When we used Cu^{2+} -phenanthroline (as opposed to bBBr), cross-linking of V49C-PLB to V89C-SERCA2a was completely inhibited by Ca^{2+} , with a K_{Ca} value of $0.48 \pm 0.09 \mu\text{M}$.

Specific Interaction of PLB with E2-ATP State of SERCA2a—In addition to requiring the Ca^{2+} -free condition, the cross-linking of PLB at cytoplasmic domain IB residues to SERCA2a is stimulated by the nucleotides, ATP or ADP (4–6). Similarly, we found that ATP stimulated the cross-linking of I45C, Cys⁴⁶, I47C, I48C, M50C, and L51C of PLB to V89C of SERCA2a by 2–3-fold (Fig. 4, left two lanes). Only cross-linkings of V49C-PLB (no ATP stimulation) and L52C-PLB (26% ATP stimulation) to V89C-SERCA2a were relatively unaffected by ATP under these cross-linking conditions (see below). Therefore, both cytoplasmic (4–6) and transmembrane domain residues of PLB appear to interact preferentially with the nucleotide-bound, E2 conformation of SERCA2a.

It is well known that the E2 conformation of SERCA2a exhibits at least two distinct activity states: one that binds nucleotide and is incapable of being phosphorylated by P_i (23, 24), and the other that is stabilized by low pH or Me_2SO , and is stoichiometrically phosphorylated by P_i (25). When SERCA2a was locked into the latter E2 state using the E2P buffer (20% Me_2SO , 0.25 mM P_i , absence of Ca^{2+}), we found that it was efficiently phosphorylated by P_i to form E2P (Fig. 4, lane 5), which drastically reduced cross-linking at all PLB domain II residues (including V49C and L52C) to V89C of SERCA2a (Fig. 4, lane 3). Inclusion of 3 mM ATP into this phosphorylation buffer virtually eliminated phosphoryl-

Transmembrane Residues of PLB Binding to E2-ATP

ation of SERCA2a by P_i (Fig. 4, lane 6), as expected from classical work with SERCA1a (23, 24), but at the same time, stimulated cross-linking of PLB to V89C of SERCA2a by 8–20-fold at all PLB residues tested, including V49C and L52C in domain II (Fig. 4, lane 4). A similar behavior was noted for cross-linking of N30C of PLB in domain IB to Lys³²⁸ of SERCA2a (Fig. 4, bottom lanes). For cross-linking of N30C of PLB to Lys³²⁸ of WT-SERCA2a, ATP stimulation was 2.2-fold in standard cross-linking buffer (*E2* buffer), as noted previously (5), but increased to 8.7-fold in buffer containing 20% Me₂SO favoring P_i phosphorylation (*E2P* buffer). All these results suggest that PLB does not bind to the *E2* state of SERCA2a that is phosphorylated by P_i and point out the utility of PLB as a reporter molecule to sense different kinetic states of SERCA2a.

We next assessed ATP binding affinities of SERCA2a in the *E2* state favoring *E2P* formation (20% Me₂SO, 0.25 mM P_i , absence of Ca²⁺). For SERCA2a co-expressed with N30C-PLB and V49C-PLB, ATP inhibited phosphorylation by P_i with K_{ATP} values of 42.4 ± 6.0 and 40.2 ± 8.8 μ M, respectively (Fig. 5, solid symbols). Similar ATP binding affinities of SERCA1a were reported previously when inhibition of P_i phosphorylation was measured (23, 24). Stimulation of cross-linking by ATP of N30C-PLB in domain IB and V49C-PLB in domain II to SERCA2a under identical conditions occurred with K_{ATP} values of 49.8 ± 5.1 and 16.6 ± 0.7 μ M, respectively (Fig. 5, open symbols). Thus, stimulation of cross-linking by ATP at two different domains of PLB occurred over the same concentration range as did inhibition of *E2P* formation by ATP, providing strong evidence that PLB only recognizes *E2*-ATP. In control experiments we observed that the cross-linking reagents themselves did not interfere with ³²P_i phosphorylation of SERCA2a, suggesting that the enzyme remained intact throughout the incubations. Moreover, the ATP binding affinities determined for inhibition of P_i phosphorylation and stimulation of cross-linking here agree with ATP binding affinities determined previously for stimulation of PLB cross-linking at Cys³¹⁸ (4) and T317C (6) of SERCA2a (determined in the absence of P_i phosphorylation), all supporting a unique state of SERCA2a that recognizes PLB (*E2*-ATP).

TG Inhibition of Cross-linking of Domain II Residues of PLB to SERCA2a—Cross-linking of domain IB residues of PLB to SERCA2a is completely prevented by the irreversible Ca²⁺ pump inhibitor, TG (4–6). Identical results were obtained by cross-linking all of the domain II mutants of PLB (I45C-L52C) to V89C of SERCA2a at M2 (Fig. 6A). TG inhibition curves are shown in Fig. 6B for the strongest cross-linking mutants, I48C-PLB, V49C-PLB, M50C-PLB, and L52C-PLB. K_i values for TG inhibition of cross-linking of I48C (0.23 ± 0.07 μ M), M50C (0.26 ± 0.04 μ M), and L52C (0.29 ± 0.02 μ M) of PLB to V89C of SERCA2a (Fig. 6B) were similar to K_i values determined previously for cross-linking of cytoplasmic domain IB residues to SERCA2a (4–6). Cross-linking of V49C-PLB to V89C-SERCA2a was somewhat less sensitive to TG, yielding a K_i value of 0.48 μ M. In the case of V49C-PLB, cross-linking with Cu²⁺-phenanthroline was also prevented by TG (data not shown), which was not reported previously (7). These unequivocal effects of TG on cross-linking at two different PLB domains suggest that TG binding to SERCA2a prevents interaction with the entire PLB molecule and contradict previous conclusions drawn from immunoprecipitation assays (26).

The lack of ATP effect on cross-linking of V49C-PLB to V89C-SERCA2a in *E2* buffer (Fig. 4, lanes 1 and 2) allowed us to test if ATP interferes with TG inhibition of cross-linking in this buffer system. Indeed, TG inhibited the cross-linking of V49C-PLB to V89C-SERCA2a with a K_i value of 0.12 ± 0.02 μ M when measured in the absence of ATP, but the K_i increased to 0.48 ± 0.07 μ M when measured in the presence of ATP (Fig. 6C). This 4-fold decrease in apparent TG affinity induced

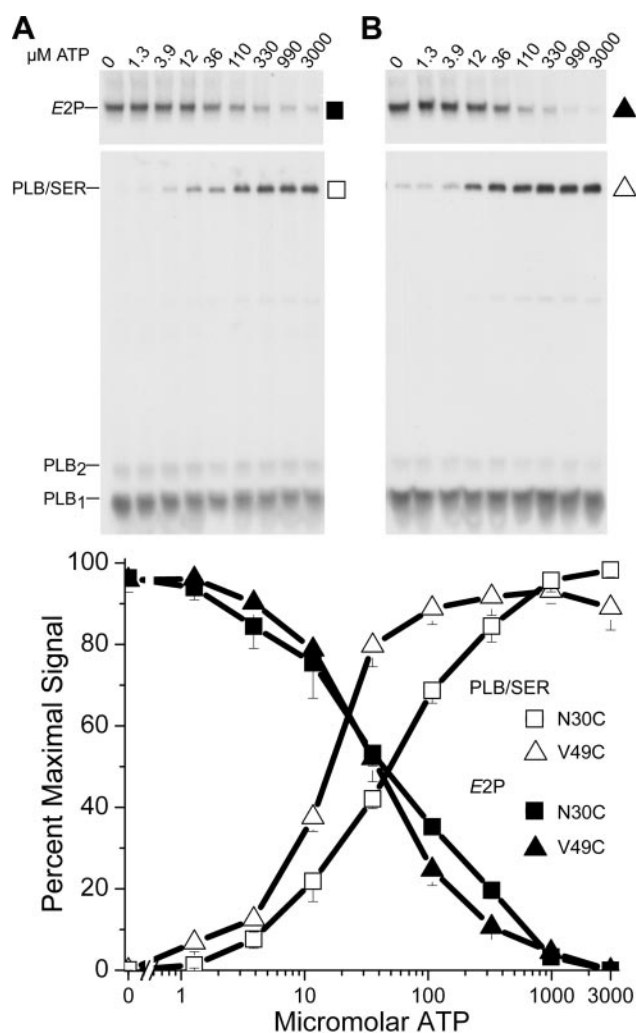


FIGURE 5. ATP concentration dependence on cross-linking and *E2P* formation. N30C-PLB co-expressed with WT-SERCA2a (A) and V49C-PLB co-expressed with V89C-SERCA2a (B) were cross-linked in *E2P* buffer as described in the legend to Fig. 4. *E2P* formation was for 10 min at room temperature, followed by addition of KMUS for 10 min for cross-linking of N30C-PLB to WT-SERCA2a, and bBBr for 1 h for cross-linking of V49C-PLB to V89C-SERCA2a. Samples were then terminated for neutral SDS-PAGE (immunoblots) or acidic LDS-PAGE (*E2P* formation). Upper autoradiograms show *E2P* formation, and middle autoradiograms show PLB cross-linked to SERCA2a. The bottom graph shows the ATP concentration dependence for stimulation of PLB cross-linking to SERCA2a (open symbols) and for inhibition of *E2P* formation (filled symbols). In the plot, baseline values obtained in the absence of ATP were set at 0 and 100% for protein cross-linking and *E2P* formation, respectively ($n = 5$).

by ATP provides further strong evidence for the competition between ATP and TG for binding to SERCA (27–29), and moreover emphasizes that PLB binds to *E2*-ATP, but not *E2*-TG (4–6).

Functional Role of Val⁴⁹ of PLB—Val⁴⁹, located three residues in from the C terminus of PLB, appears to be an important residue for physical and functional interaction with SERCA2a (7, 11, 16, 17). As demonstrated above, V49C of PLB cross-links with stoichiometric efficiency to V89C of SERCA2a from a distance of 5 Å or less. However, there are apparent conflicts in the literature regarding the functional effects of Val⁴⁹ on SERCA2a inhibition. Mutation of Val⁴⁹ to either of the two smaller conserved residues, Ala or Gly, has been reported to markedly attenuate (11, 16) or enhance (17) PLB function, respectively. To resolve these apparent inconsistencies on the functional role of Val⁴⁹, this issue was re-examined.

WT-PLB (containing native Cys residues Cys³⁶, Cys⁴¹, and Cys⁴⁶) and WT-PLB with Val⁴⁹ changed to Gly, Ala, Cys, or Leu were co-expressed

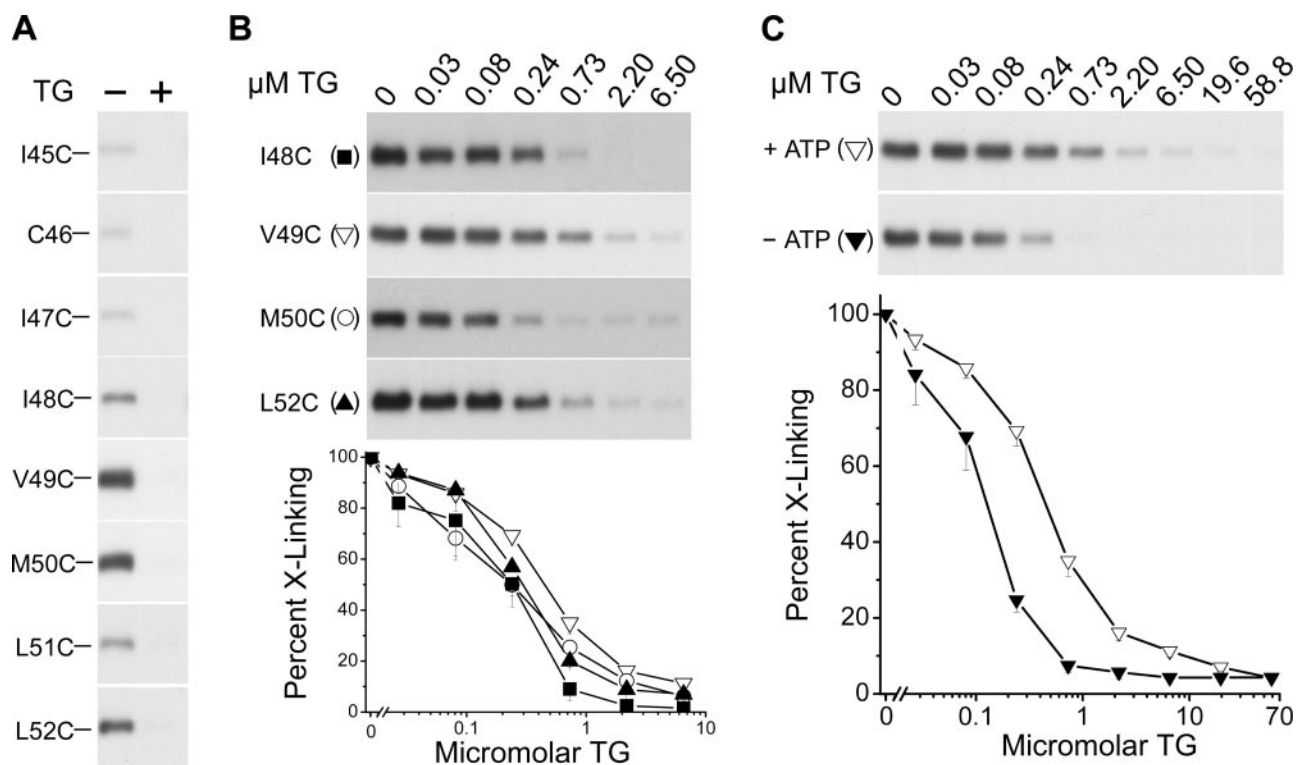


FIGURE 6. TG inhibition of cross-linking of residues 45–52 of PLB to V89C-SERCA2a. Cross-linking of the different PLB mutants to V89C-SERCA2a was conducted in E2 buffer as described in the legend to Fig. 3. *A*, cross-linking was conducted in the presence and absence of 40 μM TG. *B*, concentration dependence of TG inhibition of cross-linking. *Upper panels*, representative immunoblots for TG inhibition of cross-linking of I48C-, V49C-, M50C-, and L52C-PLB to V89C-SERCA2a. *Lower panel*, graph showing TG inhibition of cross-linking of PLB mutants, normalized to 100% for each mutant ($n = 4-6$). *C*, ATP effect on TG inhibition of cross-linking of V49C-PLB to V89C-SERCA2a. Cross-linking was conducted with bBB in the presence and absence of 3 mM ATP. *Upper panels*, representative immunoblots obtained after cross-linking with and without 3 mM ATP. *Lower panel*, graph of TG inhibition of cross-linking, determined in the presence and absence of 3 mM ATP ($n = 4$).

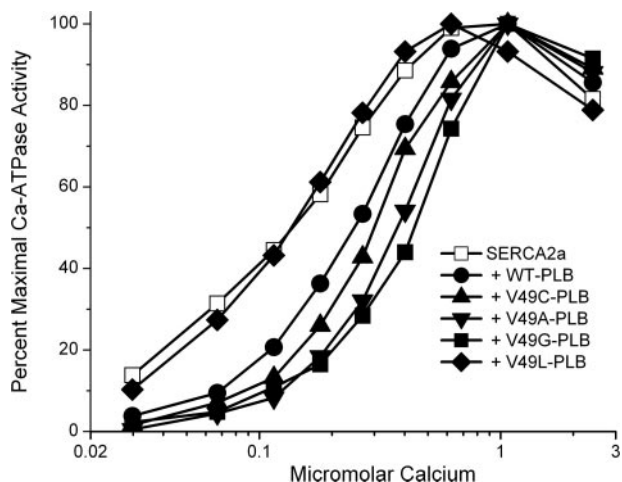


FIGURE 7. Mutational effects at Val⁴⁹ on PLB inhibitory function. Ca^{2+} -ATPase activities of WT-SERCA2a and WT-SERCA2a co-expressed with WT-PLB or the different PLB mutants indicated were measured. All PLB mutations were made on the WT-PLB background.

with WT-SERCA2a in insect cell microsomes and effects on Ca^{2+} activation of Ca^{2+} -ATPase activity were measured (Fig. 7). It is apparent that V49G-PLB, V49A-PLB, and V49C-PLB all decreased SERCA2a apparent Ca^{2+} affinity as well, or even better, than WT-PLB. All gave large rightward shifts in Ca^{2+} activation profiles of Ca^{2+} -ATPase activity. Only the V49L-PLB mutant, containing a mutated residue with a longer hydrophobic side chain, failed to inhibit SERCA2a activity significantly. Similar results were obtained when Ca^{2+} transport was measured (data not shown). Table 2 demonstrates that both V49A-PLB and V49G-PLB are supershifters (11) of Ca^{2+} -ATPase activity, increas-

TABLE 2

PLB mutational effects at Val⁴⁹ on apparent Ca^{2+} affinity of SERCA2a

WT-SERCA2a was co-expressed with WT-PLB or PLB with residue substitutions at Val⁴⁹ as indicated. Ca^{2+} -ATPase activities were measured, and K_{Ca} values (μM) for Ca^{2+} activation of ATP hydrolysis are reported. All PLB mutations were made on the WT-PLB background (Cys³⁶, Cys⁴¹, and Cys⁴⁶ unchanged). Results are the means \pm S.D. from three to six preparations.

Protein expressed	K_{Ca} values	
	- Antibody	+ Antibody
	μM	
WT-SERCA2a	0.14 ± 0.02	0.14 ± 0.02
+ WT-PLB	0.24 ± 0.02	0.15 ± 0.02
+ V49G-PLB	0.44 ± 0.02	0.22 ± 0.02
+ V49A-PLB	0.36 ± 0.02	0.18 ± 0.02
+ V49C-PLB	0.27 ± 0.02	0.16 ± 0.02
+ V49L-PLB	0.15 ± 0.01	0.12 ± 0.01

ing the K_{Ca} values relative to WT-PLB by 50% or more when co-expressed with SERCA2a. PLB inhibition by all active mutants was greatly attenuated by the anti-PLB antibody, as observed previously for WT-PLB and other supershifting PLB mutants (13, 14, 30) (Table 2). Thus, V49A-PLB is actually a gain of function mutant, not a loss of function mutant, as originally reported (11). A previous study, using V49A-PLB as a dominant-negative tool to ablate WT-PLB function in failed cardiac myocytes should therefore be viewed skeptically (16). However, the results of Table 2 are consistent with the ability of V49G-PLB to induce heart failure when overexpressed in transgenic mouse hearts (17).

DISCUSSION

In this study, we extended our cross-linking approach to probe molecular interactions between domain II of PLB and the transmembrane domain of SERCA2a. We demonstrated that different PLB

Transmembrane Residues of PLB Binding to E2-ATP

mutants with Cys substitutions at residues 45–52 were all able to cross-link to V89C of SERCA2a, but from different distances (0 to 10 Å), with different time courses, and with efficiencies up to 100%. Like our earlier studies at PLB domain IB (4–6), cross-linking at this second major PLB domain indicates that PLB only interacts with SERCA2a in the Ca²⁺-free, E2 conformation. This interaction is augmented by bound nucleotide, but prevented by TG and phosphorylation of SERCA2a to form the E2P state. As in previous studies, conditions that favor cross-linking of PLB and SERCA2a are strongly correlated with those that support inhibition of Ca²⁺ transport, suggesting that SERCA2a regulation depends on dynamic equilibrium between bound and free PLB.

Ca²⁺ Effect on PLB/SERCA2a Association—Taken together with previous studies on cross-linking cytoplasmic residues of PLB to SERCA2a (4–6), our current results support a global dissociation of the entire PLB molecule from SERCA2a upon binding Ca²⁺. Specifically, inhibition of cross-linking between two distinct domains of PLB (IB and II) and two different regions of SERCA2a (cytoplasmic extension of M4 and M2) was in all cases strongly correlated with concentrations of Ca²⁺ required to activate the reaction cycle of SERCA2a. This observation is consistent with many reports showing that PLB has no effect on SERCA2a when the enzyme is maximally activated by Ca²⁺ (1). Nevertheless, two groups have recently suggested that PLB remains bound to SERCA2a throughout the reaction cycle (31, 32). Both groups used fluorescence probes to study the purified skeletal muscle Ca²⁺ pump (SERCA1a) reconstituted with bacterially expressed (31) or synthetic (32) PLB. Both groups concluded that the two proteins did not dissociate when the Ca²⁺ pump bound Ca²⁺. They pointed out that local domain motion near Lys³²⁸ of SERCA2a could account for the failure of N30C-PLB to cross-link to SERCA upon binding Ca²⁺ (5), and that PLB need not necessarily dissociate from SERCA2a to account for the failure of cross-linking. However, this potential caveat seems improbable given that three different residues of PLB in domain IB (N27C, N30C, and L31C) all failed to cross-link to three separate residues of SERCA2a (T317C, Cys³¹⁸, and Lys³²⁸) when the high affinity Ca²⁺-binding sites were occupied (4–6). Furthermore, we now report identical Ca²⁺ effects for a completely different region of PLB and SERCA2a: the C-terminal transmembrane domain of PLB and M2 of SERCA2a. This new region is 30–40 Å away from domain IB of PLB and the cytoplasmic extension of M4 discussed above. Thus, it is very unlikely that “steric hindrance” or “changes in orientation” of individual SERCA residues in the presence of Ca²⁺ (31, 32) could account for the total failure of PLB cross-linking at all sites and residues tested to date (4–6). Furthermore, our use of cross-linking agents spanning distances from 0 to 15 Å (4–6) and the high efficiency of cross-linking in the absence of Ca²⁺, make it equally unlikely that small shifts in residue distances induced by Ca²⁺ binding to SERCA2a could account for the complete abolition of cross-linking at all sites when the Ca²⁺-binding sites are occupied, as has also been suggested (31, 32). It should be pointed out that our cross-linking results have been obtained after co-expression of PLB and SERCA2a in cellular membranes, where they are expected to adopt their physiological orientations and have been shown to be well coupled functionally (Tables 1 and 2) (13). On the other hand, reconstituted membrane proteins tend to produce mixed orientations, and introduction of a fluorescence probe into a purified PLB molecule reports on the local environment, which may or may not be sensitive to specific protein-protein interactions (31, 32). Because the PLB molecules used in these fluorescence studies (31, 32) are likely to form larger aggregates in lipid bilayers (4, 14, 33), nonspecific interactions between the PLB molecules themselves also cannot be ruled out.

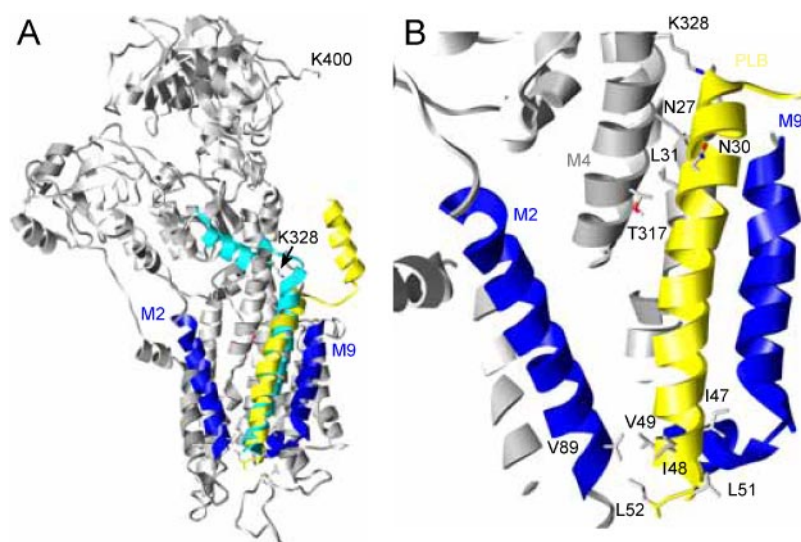
Key Role of ATP-stabilized E2 Conformation—Cross-linking of PLB at cytoplasmic domain IB is stimulated by ATP binding to the N-domain of SERCA2a, suggesting that ATP binding induces a global conformational change that is sensed by PLB (4–6). In this study, we further showed that cross-linking at transmembrane domain II of PLB to V89C-SERCA2a is also stimulated by ATP, illustrating that this conformational change most likely involves the entire SERCA2a molecule. The SERCA2a E2 conformation that binds PLB has relatively high affinity for ATP (20–30 μM) (4), and this stimulation is therefore relevant to conditions experienced within the cell. As originally pointed out by McIntosh and Boyer (24), Ca²⁺-ATPase has bound nucleotide during most or all steps of the catalytic cycle; furthermore, it is well known that ATP plays an important role in stimulating the transition from E2 to E1·Ca²⁺, one of the rate-limiting steps in the overall reaction cycle (8, 34).

All of these observations help to explain how PLB inhibits the Ca²⁺ pump at the molecular level. We propose that when a PLB monomer binds to SERCA2a in the E2·ATP state, the enzyme becomes immobilized in that specific conformation. Progression of the catalytic cycle then remains blocked until PLB dissociates from SERCA2a, allowing the enzyme to transition from E2 to E1, thereby forming the high affinity Ca²⁺-binding sites, which bind Ca²⁺ with micromolar affinity and initiate the transport cycle. Thus, at any given time there will be two distinct populations of SERCA2a molecules, one inhibited population with PLB bound to the E2·ATP state, and a second population free from PLB and pumping at a normal rate. In steady state measurements of ATP hydrolysis or Ca²⁺ transport, the effect of the competition between PLB and Ca²⁺ for binding to two different states of SERCA2a will be an apparent decrease in Ca²⁺ affinity of SERCA2a (8), which is the hallmark of PLB regulation (1).

When SERCA is in the E2 conformation, it was previously shown that ATP competes for P_i phosphorylation, with an apparent nucleotide affinity around 50 μM (23, 24). Similar nucleotide affinities are observed for ATP stimulation of PLB cross-linking at domain IB (4–6), and at domain II of PLB (reported here). In the current study, P_i phosphorylation of E2 strongly inhibited cross-linking to the Ca²⁺ pump, indicating that E2P has its own unique conformation and confirming that PLB binds primarily to the E2 conformation that is stabilized by nucleotides. This effect was reversed by ATP binding to E2, presumably due to its competition with P_i phosphorylation. Again, we view this competition as producing two populations of SERCA2a, either bound to PLB, or available for formation of E2P, and that the molecules that are cross-linked (PLB/SER) in the gels in Fig. 5 are therefore distinct from those labeled by ³²P_i (E2P). Inhibition of PLB cross-linking by TG is also consistent with this idea, because TG competes for ATP binding to the E2 state (29). Thus, the results illustrate that cross-linking PLB can distinguish different E2 conformations, namely E2·ATP, which recognizes PLB, and E2·TG or E2P, which apparently cannot bind PLB.

Effect of TG on PLB/SERCA2a Interactions—The E2 conformation of SERCA2a inhibited by TG appears to be incapable of binding PLB. TG binds to SERCA1a between M3, M5, and M7 and has been shown to form a dead-end complex with the Ca²⁺ pump, which has properties resembling E2 (35, 36) and has proven very amenable to crystallization (34). Like our previous results with domain IB of PLB, we found that TG prevented cross-linking of PLB domain II to SERCA2a at all residues analyzed, thus contradicting conclusions drawn from a previous immunoprecipitation study (26). For both domain IB and domain II, the concentration dependence of TG inhibition of cross-linking was nearly stoichiometric with the concentration of Ca²⁺ pumps used in the cross-linking assay (4–6), confirming that TG binds essentially irreversibly, in a one to one molar ratio to the Ca²⁺-ATPase (27, 37, 38). Nonetheless,

FIGURE 8. Structural model for the interaction between PLB and SERCA. *A*, two independent structures for PLB were docked next to the structure of the E2 state of SERCA bound to TG (36). The cyan PLB was derived from a monomeric mutant (43), whereas the yellow PLB was extracted from the pentameric structure of a construct corresponding to the WT human sequence (44). The transmembrane helices in both PLB structures are similar and allow cross-linked residues to be positioned at a reasonable distance. However, the cytoplasmic domains go in completely different directions, suggesting an innate flexibility in the loop that connects PLB domains IA and IB. *B*, close up of the cross-linked residues investigated in this and previous studies. The C terminus of PLB is wedged between the luminal end of M2 and a loop between M9 and M10 of SERCA (colored blue), suggesting that M2 must move to accommodate PLB binding and that Val⁴⁹ controls access to this binding site. The figure identifies Asn²⁷ for consistency with the text, although this residue is actually Lys in the construct used for this particular structure. Figure was made with Chimera.



with use of V49C-PLB cross-linking to V89C-SERCA2a, we were able to show that ATP could compete for TG inhibition of cross-linking, shifting the K_i value for TG inhibition from 0.12 to 0.48 μM . Also, in the presence of ATP, cross-linking of V49C-PLB to V89C-SERCA2a was about 2-fold less sensitive to TG than cross-linking at the other domain II sites of PLB analyzed (Fig. 6). These results suggest that V49C-PLB and ATP act synergistically to stabilize a state of SERCA2a that is partially resistant to inhibition by TG.

Role of Val⁴⁹ in PLB/SERCA2a Interactions—The close proximity and highly efficient cross-linking interaction between V49C of PLB and V89C of SERCA2a strongly suggest an important functional role for Val⁴⁹ of PLB. Indeed, when Val⁴⁹ is substituted with smaller amino acids (Ala, Gly, or Cys), functional interaction with SERCA2a is enhanced, whereas the large, bulky side chain of Leu abolishes this interaction. Thus, Val⁴⁹ may provide access control for binding of PLB to SERCA2a. According to this hypothesis, when Val⁴⁹ is replaced by a small residue, PLB fits better into its binding pocket next to M4 on SERCA2a, which enhances the inhibition. This may explain why cross-linking between V49C-PLB and V89C-SERCA2a with bBBr is nearly complete and independent of ATP, unlike Cys mutations at neighboring residues (Fig. 4). Specifically, the higher affinity of V49C-PLB for SERCA2a could override the conformational effect of ATP, perhaps by producing the relevant conformation of SERCA2a even in the absence of nucleotide. This conformational effect could also explain why cross-linking V49C is more resistant to TG, whose binding is antagonized by the ATP-bound conformation of SERCA2a (Fig. 6).

Structural Considerations—To understand such conformational effects, it would be highly desirable to have a structural model for the interaction between PLB and SERCA2a. However, this is not straightforward given the available atomic structures for the two molecules. In the case of SERCA, all available structures of the E2 conformation have been determined in the presence of TG (34, 39, 40). As a result, the structure of the transmembrane domains are virtually identical, even though differences would be expected for the E2 state versus the E2P state. Furthermore, the E2P state containing the low affinity Ca²⁺-binding sites has recently been shown to be incompatible with TG binding (40) and, as shown here and in our earlier work (4–6), the E2-ATP state that binds PLB also apparently excludes TG. Thus, we can probably expect structural differences in the absence of TG and certainly can expect differences in the nucleotide-bound conformation that interacts with PLB. Unfortunately, we have no reliable way to predict what these differences might be.

In the case of PLB, although an α -helical transmembrane domain has long been predicted (12, 41), and now confirmed in several NMR studies using different conditions, the structure of the highly charged, cytoplasmic domain has been extremely variable (42–45). It is plausible that the cytoplasmic domain is sensitive to its environment (1) and adopts a unique structure upon binding to SERCA2a (46). Again, we have no reliable way to know what this structure might be. Thus, the model in Fig. 8 is meant to show the juxtaposition of residues identified through our cross-linking studies, without representing a precise atomic model for the regulatory interaction between these two molecules. For this model, we have used the SERCA1a structure bound to TG in the E2 conformation (36) and two recent structures of PLB in dodecylphosphocholine micelles (43, 44).

The region of Val⁸⁹-SERCA and Val⁴⁹-PLB is of primary relevance to the current work. Unlike a recent model of PLB bound to SERCA, which showed an unraveling of the PLB helix near its C terminus (7), this structure continues as an intact helix all the way through Leu⁵². This continuous helix is consistent with our cross-linking results: in particular, with the equivalent cross-linking efficiency of V49C and L52C of PLB to V89C-SERCA2a and the much weaker cross-linking of intervening residues with the shorter length cross-linking reagents, bBBr and Cu²⁺-phenanthroline. Furthermore, the stronger cross-linking of L50C-PLB with the longer reagent BMH is consistent with Leu⁵⁰ (*not visible*) occupying a position on the opposite side of the helix; Val⁴⁹ may be blocking cross-linking of other residues (*e.g.* I47C and I48C) in a similar position, or these residues may be interacting with a different structural element of SERCA (see below).

The model shows a narrow constriction in the vicinity of Val⁸⁹ of SERCA, supporting the idea that the size of residue 49 of PLB could control access of PLB to its binding site. This constriction may explain why shortening the side chain of residue 49 could make PLB a more effective inhibitor (Fig. 8), in contrast to earlier results suggesting that a long side chain at residue 49 is required for PLB binding (7) and that PLB loses inhibitory function when Val⁴⁹ is changed to Ala (11, 16). This constriction is bounded by the luminal end of M2 and a short helix in the luminal loop between M9 and M10 (both blue in Fig. 8). As positioned in the E2-TG structure for SERCA, there is not enough space for PLB to fit between these two structural elements, indicating that these elements must move apart. The structure of M7 through M10 is generally considered to be static, showing almost no change in the various structures of SERCA throughout the reaction cycle. Therefore, it seems more likely that M2 would be the moveable element. Indeed, compari-

Transmembrane Residues of PLB Binding to E2-ATP

son of E2·TG with E1·Ca₂ reveals dramatic changes in M2 (39), which have plausibly been proposed as responsible for pushing PLB out of its binding site upon Ca²⁺ binding by SERCA (7). On the one hand, TG binds in a pocket between M3, M4, and M7 and there is no obvious way for it to directly affect the position of M2, which is located on the opposite side of the transmembrane domain. On the other hand, ATP could exert its effect on PLB by binding to the cytoplasmic N-domain and altering its association with the A-domain, which is directly connected to the top of the M2 helix. Thus, M2 provides a plausible path for coupling the binding of ATP to PLB affinity.

At the cytoplasmic side of the membrane, both PLB structures solved in dodecylphosphocholine micelles (43, 44) can be oriented such that the cross-linked residues (Asn²⁷, Asn³⁰, and Leu³¹) are within reasonable range of the corresponding SERCA residues (Lys³²⁸, Cys³¹⁸, and Thr³¹⁷) (4–6). However, the two structures differ markedly in the orientation of their cytoplasmic domains. In the WT-PLB structure shown in Fig. 8, the N-terminal helix is too far away to interact with SERCA (yellow) (44), whereas in the monomeric C41F structure (cyan) (43), this helix runs right through the middle of the M4 helix of SERCA. This suggests an innate flexibility in the unstructured loop that connects PLB domain IA to the rest of the molecule. As has been pointed out before (5, 6), it is impossible for the N terminus of PLB to reach the KDDK⁴⁰⁰ loop on SERCA that was implicated in an earlier cross-linking study (47), but which has proven unreproducible with our cross-linking reagents. Instead, it seems likely that the N-terminal helix binds to some other surface in the “stalk” region of SERCA2a (e.g. extensions of M4 and M5 and the M6/M7 loop). It will be the goal of future studies to define these interactions, either by cross-linking or by direct structural investigations.

Acknowledgments—We thank Jin Guo and Glen Schmeisser for technical assistance.

REFERENCES

1. Simmerman, H. K., and Jones, L. R. (1998) *Physiol. Rev.* **78**, 921–947
2. Haghghi, K., Gregory, K. N., and Kranias, E. G. (2004) *Biochem. Biophys. Res. Commun.* **322**, 1214–1222
3. Young, H. S., and Stokes, D. L. (2004) *J. Membr. Biol.* **198**, 55–63
4. Jones, L. R., Cornea, R. L., and Chen, Z. (2002) *J. Biol. Chem.* **277**, 28319–28329
5. Chen, Z., Stokes, D. L., Rice, W. J., and Jones, L. R. (2003) *J. Biol. Chem.* **278**, 48348–48356
6. Chen, Z., Stokes, D. L., and Jones, L. R. (2005) *J. Biol. Chem.* **280**, 10530–10539
7. Toyoshima, C., Asahi, M., Sugita, Y., Khanna, R., Tsuda, T., and MacLennan, D. H. (2003) *Proc. Natl. Acad. Sci. U. S. A.* **100**, 467–472
8. Cantilina, T., Sagara, Y., Inesi, G., and Jones, L. R. (1993) *J. Biol. Chem.* **268**, 17018–17025
9. Toyofuku, T., Kurzydowski, K., Tada, M., and MacLennan, D. H. (1994) *J. Biol. Chem.* **269**, 3088–3094
10. Kimura, Y., Asahi, M., Kurzydowski, K., Tada, M., and MacLennan, D. H. (1998) *J. Biol. Chem.* **273**, 14238–14241
11. Kimura, Y., Kurzydowski, K., Tada, M., and MacLennan, D. H. (1997) *J. Biol. Chem.* **272**, 15061–15064
12. Simmerman, H. K., Kobayashi, Y. M., Autry, J. M., and Jones, L. R. (1996) *J. Biol. Chem.* **271**, 5941–5946
13. Autry, J. M., and Jones, L. R. (1997) *J. Biol. Chem.* **272**, 15872–15880
14. Cornea, R. L., Autry, J. M., Chen, Z., and Jones, L. R. (2000) *J. Biol. Chem.* **275**, 41487–41494
15. Toyoshima, C., and Mizutani, T. (2004) *Nature* **430**, 529–535
16. Minamisawa, S., Hoshijima, M., Chu, G., Ward, C. A., Frank, K., Gu, Y., Martone, M. E., Wang, Y., Ross, J., Jr., Kranias, E. G., Giles, W. R., and Chien, K. R. (1999) *Cell* **99**, 313–322
17. Haghghi, K., Schmidt, A. G., Hoit, B. D., Brittsan, A. G., Yatani, A., Lester, J. W., Zhai, J., Kimura, Y., Dorn, G. W., 2nd, MacLennan, D. H., and Kranias, E. G. (2001) *J. Biol. Chem.* **276**, 24145–24152
18. Porzio, M. A., and Pearson, A. M. (1977) *Biochim. Biophys. Acta* **490**, 27–34
19. Lichtner, R., and Wolf, H. U. (1979) *Biochem. J.* **181**, 759–761
20. Sham, J. S., Jones, L. R., and Morad, M. (1991) *Am. J. Physiol.* **261**, H1344–H1349
21. Green, N. S., Reisler, E., and Houk, K. N. (2001) *Protein Sci.* **10**, 1293–1304
22. Napier, R. M., East, J. M., and Lee, A. G. (1987) *Biochim. Biophys. Acta* **903**, 374–380
23. Masuda, H., and de Meis, L. (1973) *Biochemistry* **12**, 4581–4585
24. McIntosh, D. B., and Boyer, P. D. (1983) *Biochemistry* **22**, 2867–2875
25. de Meis, L., Martins, O. B., and Alves, E. W. (1980) *Biochemistry* **19**, 4252–4261
26. Asahi, M., McKenna, E., Kurzydowski, K., Tada, M., and MacLennan, D. H. (2000) *J. Biol. Chem.* **275**, 15034–15038
27. Inesi, G., and Sagara, Y. (1992) *Arch. Biochem. Biophys.* **298**, 313–317
28. McIntosh, D. B., Woolley, D. G., Vilsen, B., and Andersen, J. P. (1996) *J. Biol. Chem.* **271**, 25778–25789
29. DeJesus, F., Girardet, J. L., and Dupont, Y. (1993) *FEBS Lett.* **332**, 229–232
30. Autry, J. M., and Jones, L. R. (1998) *Ann. N. Y. Acad. Sci.* **853**, 92–102
31. Li, J., Bigelow, D. J., and Squier, T. C. (2004) *Biochemistry* **43**, 3870–3879
32. Mueller, B., Karim, C. B., Negrashov, I. V., Kutchai, H., and Thomas, D. D. (2004) *Biochemistry* **43**, 8754–8765
33. Hughes, E., Clayton, J. C., and Middleton, D. A. (2005) *Biochemistry* **44**, 4055–4066
34. Moller, J. V., Nissen, P., Sorensen, T. L.-M., and le Maire, M. (2005) *Curr. Opin. Struct. Biol.* **15**, 387–393
35. Inesi, G., and Sagara, Y. (1994) *J. Membr. Biol.* **141**, 1–6
36. Toyoshima, C., and Nomura, H. (2002) *Nature* **418**, 605–611
37. Sagara, Y., and Inesi, G. (1991) *J. Biol. Chem.* **266**, 13503–13506
38. Kijima, Y., Ogunbunmi, E., and Fleischer, S. (1991) *J. Biol. Chem.* **266**, 22912–22918
39. Toyoshima, C., and Inesi, G. (2004) *Annu. Rev. Biochem.* **73**, 269–292
40. Picard, M., Toyoshima, C., and Champeil, P. (2006) *J. Biol. Chem.* **281**, 3360–3369
41. Simmerman, H. K., Collins, J. H., Theibert, J. L., Wegener, A. D., and Jones, L. R. (1986) *J. Biol. Chem.* **261**, 13333–13341
42. Lamberth, S., Schmid, H., Munchbach, M., Vorherr, T., Krebs, E., Carafoli, E., and Griesinger, C. (2000) *Helv. Chim. Acta* **83**, 2141–2152
43. Zamoon, J., Mascioni, C. A., Thomas, D. D., and Veglia, G. (2003) *Biophys. J.* **85**, 2589–2598
44. Oxenoid, K., and Chou, J. J. (2005) *Proc. Natl. Acad. Sci. U. S. A.* **102**, 10870–10875
45. Andronesi, O. C., Becker, S., Seidel, K., Heise, H., Young, H. S., and Baldus, M. (2005) *J. Am. Chem. Soc.* **127**, 12965–12974
46. Kirby, T. L., Karim, C. B., and Thomas, D. D. (2004) *Biochemistry* **43**, 5842–5852
47. James, P., Inui, M., Tada, M., Chiesi, M., and Carafoli, E. (1989) *Nature* **342**, 90–92